International Journal of Heat and Mass Transfer 55 (2012) 2384–2393

Contents lists available at SciVerse ScienceDirect

International Journal of Heat and Mass Transfer

journal homepage: www.elsevier.com/locate/ijhmt

Temperature distribution and local heat flux in the unidirectional freezing of antifreeze-protein solution

Yoshimichi Hagiwara *, Daichi Yamamoto

Department of Mechanical and System Engineering, Graduate School of Science and Technology, Kyoto Institute of Technology, Matsugasaki, Sakyo-ku, Kyoto 606-8585, Japan

ARTICLE INFO

Article history:
Received 18 February 2011
Received in revised form 10 January 2012
Accepted 11 January 2012
Available online 8 February 2012

Keywords:
Local heat flux
Near-infrared camera
Winter flounder antifreeze protein
Ice/solution interface
Fluorescence microscopy

ABSTRACT

Experiments have been conducted on the unidirectional freezing of dilute aqueous solutions of winter flounder antifreeze protein, which are 0.02 mm thick, between two cover glasses on the stage of a microscope. The instantaneous temperature field has been obtained by measuring the intensity of near-infrared light with a near-infrared camera. In addition, the local protein concentration has been measured separately using the brightness of fluorescence emitted from molecules tagged to the protein. It is found that the temperature distribution in the ice region near the ice/water interface is similar to that predicted from the modified Neumann solution. Furthermore, the temperature measurement made using the near-infrared light with a specific wavelength is verified. In addition to this, in the case of antifreeze protein solutions, serrated interfaces are observed. The sum of the conduction heat flux of a protein solution near the front edge of the serrated interface and the heat flux for solidification is lower than the conduction heat flux of ice. On the other hand, the sum of the conduction heat flux of protein solution near the bottom edge of the serrated interface and the heat flux for solidification is higher than the conduction heat flux of ice. The balance of heat flux is obtained by taking account of heat convection due to high-concentration regions of protein. These regions move to the deepest parts of the interface and form narrow liquid regions inside the ice. The convection is maintained by the heat conduction in a direction perpendicular to the direction of ice growth. Not only protein adsorption to the interface but also the heat conduction/convection contributes to the modification of ice growth in the non-equilibrium state.

1. Introduction

The inhibition of ice crystal growth has been a recent focus of research for not only chemists and biochemists but also engineers. This inhibition is important in many diverse fields, including cryosurgery [1], the storage of organs for transplantation [2], the storage of tissues and cells in tissue engineering, the production of micro-ice slurries used to cool the brain during cardiac arrest, the reduction of additives without changing taste in frozen foods [3], and lowering energy costs associated with freezing and thawing foods.

One of the most promising methods for the inhibition of ice crystal growth is to use additives that affect the freezing, such as antifreeze protein (AFP). AFP lowers the temperature at which a seed crystal grows, but does not alter the temperature at which the crystal is stable during the melting process in the cases of the very low cooling rates mentioned below. Ice crystal growth might be more readily controlled by keeping the cells, tissues, organs or foods at a certain temperature between these two temperatures. Furthermore, AFP does not significantly increase osmotic pressure.

The properties of winter flounder AFP, which is among many antifreeze proteins discovered so far, have been measured widely. The measurements of the ice crystal growth and ice surface morphology in the solution of this protein are classified into two types according to the cooling rates: (i) measurements made with a very low cooling rate ($\leqslant -1$ °C/min) and (ii) measurements made with a low cooling rate (>-1.5 °C/min). In the case of the first type, an AFP solution of approximately 0.01 mm^3 (10 nanolitres) in oil or liquid paraffin was rapidly frozen at -40 °C in nanolitre osmometers [4,5]. The temperature of the frozen sample was gradually raised at 0.5 °C/min until only a single crystal approximately 7 μm in diameter remained. The solution with the tiny crystal was kept for 1 min at this temperature to allow the crystal to stabilize. This temperature was considered the 'melting point'. The solution with the crystal was gradually cooled at -1.0 °C/min. Chao et al. [6] considered that the 'freezing point' was the temperature at which the ice crystal growth velocity is higher than 0.2 μm/s. The heat flux for solidification q_{ls} was 0.061 kW/m^2 in their experiment. The thermal hysteresis, defined by the difference between the 'melting point' and the 'freezing point', was found to increase with an

* Corresponding author. Tel.: +81 75 724 7324; fax: +81 75 724 7300.
E-mail address: yoshi@kit.ac.jp (Y. Hagiwara).

0017-9310/$ - see front matter © 2012 Elsevier Ltd. All rights reserved.
doi:10.1016/j.ijheatmasstransfer.2012.01.024

Nomenclature

A	absorbance
B	brightness
C	specific heat (J/kg K)
c	concentration (kg/m^3)
h	heat transfer coefficient (W/m^2 K)
I	light intensity
k	thermal conductivity (W/m K)
L_{ls}	latent heat of fusion (J/kg)
Nu	Nusselt number
q	heat flux (W/m^2)
R	similarity variable
Ra	Rayleigh number
T	temperature (°C)
t	time (s)
u_i	interface velocity (m/s)
X	position in direction of ice growth (m)
Y	position in direction perpendicular to ice growth (m)

Greek symbols

α	thermal diffusivity (m^2/s)
ΔA	absorbance difference
δ	thickness (m)
λ	wavelength (m)
ξ	location of ice/water interface (m)
ρ	density (kg/m^3)

increase in the AFP concentration, to a point after which no further hysteresis is found [4,6].

Although the thermal hysteresis obtained by the osmometers is useful, the very low cooling rate differs from the typical cooling rates for the cryopreservation of cells (−1 °C/min to −10 °C/min) [7] and cryosurgery (−10 °C/min) [8]. The ice growth speed concerning cryosurgery was in the range of 0.013–0.051 mm/s [9]. The value for q_{ls} was estimated to be in the range of 4.1–16 kW/m^2. Because of these differences in the cooling rates and heat fluxes, experimental results for higher rates of cooling or ice growth are necessary to elucidate the activities of AFP.

In the case of the second type of cooling, there are several experimental methods that help elucidate the activities of AFP. Wilson et al. [10] used an automated lag-time apparatus. A 200 mm^3 sample solution of winter flounder AFP was held in a glass tube. The heat flux for solidification in the case of heterogeneous nucleation was estimated to be 0.13 kW/m^2 from the cooling rate, the cross section of tube and the nucleation rate. Coger et al. [11] measured the velocity and morphology of the ice/solution interface during the unidirectional freezing of 20-mm^3 solution of winter flounder AFP between two glass plates using successive images recorded by a video camera attached to a microscope. Part of the lower plate was in contact with a warm block, while part of the plate was in contact with a cool block. The heat flux necessary for solidification q_{ls} was in the range of 0–27 kW/m^2. Furukawa et al. [12] measured the velocity of serrated interfaces in similar unidirectional freezing of a 73-mm^3 solution of antifreeze glycoprotein. In their case, the heat flux necessary for solidification was in the range of 0.92–3.4 kW/m^2. However, local temperature was not measured in these studies.

Our research group previously conducted experiments on the unidirectional freezing of a 20-mm^3 solution of winter flounder AFP in a narrow gap (0.02 mm) between two cover glasses [13]. We measured the shape and velocity of the ice/liquid interface in a manner similar to that employed by Coger et al. [11] and Furukawa et al. [12]. Additionally, we obtained an average temperature over a small circular region of 0.036 mm in diameter, fixed in the observation area, by measuring the intensity of near-infrared (NIR) light using a spectrometer. When the front edges of the serrated interface (the most advanced points in the interface in the ice growth direction) happened to reach the circular region, we defined the temperature of the front edges. Similarly, when the bottom edges (the innermost parts in the ice growth direction) happened to reach the circular region, we defined the temperature of the bottom edges. The heat flux for solidification was in the range of 0.92–1.8 kW/m^2. It was found that the temperature difference between the front and bottom edges was proportional to the distance between the front and bottom edges. The instantaneous temperature field could not be measured using the spectrometer because of one-point measurement. Thus, the heat flux could not be obtained. A multi-point measurement is necessary to evaluate the thermal field and heat flux.

In the present study, we measure the instantaneous, two-dimensional temperature distribution for pure water or the winter flounder AFP solution by measuring the intensity distribution of NIR light using an NIR camera. We discuss the principle of the temperature measurement method. We compare the profile of temperature measured near the ice/water interface with the profile predicted with the unsteady conduction equation with solidification. Later in the article, we discuss the heat fluxes near the ice/water and ice/AFP-solution interfaces, obtained from the temperature distribution. To discuss the imbalance of heat flux at the ice/AFP-solution interface, we estimate the local concentration of AFP employing fluorescence microscopy [14,15]. We also discuss

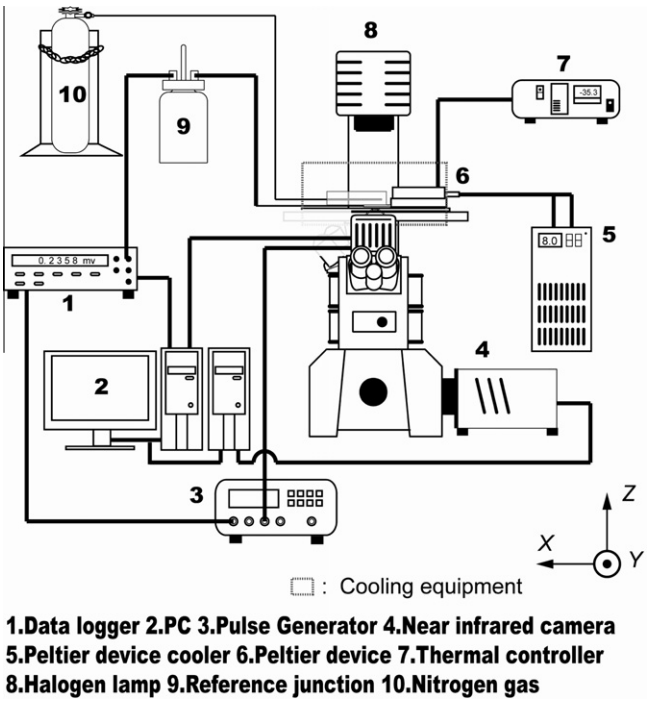

Fig. 1. Apparatus. The observation area was 0.430 × 0.340 mm^2. The pixel resolution of the near-infrared camera was 1.34 × 1.33 μm^2 and the frame rate was 1 fps. The near-infrared camera was replaced with a video camera in the case of fluorescence microscopy. In this case, the observation area was 0.392 × 0.299 mm^2. The pixel resolution of the video camera was 0.292 × 0.292 μm^2 and the frame rate was 1 fps.